

Quantum speedmeter and laser interferometric gravitational-wave antennae

F.Ya.Khalili

Abstract

A new topology of laser interferometric gravitational-wave antenna is considered. It is based on two schemes: *quantum speedmeter* and *zero-area Sagnac interferometer* and allows to obtain sensitivity better than the Standard Quantum Limit in wide band without any large-scale modifications of the standard topology of the laser interferometric antennae.

1 Introduction

It is well known that the only variables that can be continuously monitored with arbitrary high precision are the Quantum Non-Demolition (QND) observables that are the variables which operators (in the Heisenberg picture) commute with themselves at different moments of time [1, 2, 3]. A free mass has two such variables: momentum p and variable with explicit time dependence $x - pt/m$. In both cases the meter must be able to “see” momentum of free mass. However, implementation of such meters at the quantum level of sensitivity does not seem possible for the contemporary level of technology.

In the article [4] it was proposed to measure velocity of a free test mass instead of momentum. Velocity is not a true QND observable, and it is perturbed by the meter during such a measurement. However, its properties are close to properties of the momentum and therefore the perturbation can be rather easily excluded from the output signal of the meter using cross-correlation between the measurement noise and back-action noise (see details in the next section). It was shown also in the article [4] that velocity can be measured using pairs of position measurements separated by small time τ . The main requirement for such a procedure is that decoherence of the quantum state of the meter between these two measurements must be sufficiently small:

$$\tau_{\text{decoh}} \gg \Omega_{\text{signal}}^{-1}, \quad (1)$$

where τ_{decoh} is the decoherence time and Ω_{signal} is the characteristic frequency of the signal.

In the article [4] two schemes of velocity measurement were proposed: a simple semi-gedanken scheme close to the one considered in the next section and the scheme based on two coupled microwave cavities. In the article [5] it was proposed to use the second one as a local meter in the intracavity topology of laser gravitational-wave antennae and it was shown that it allows to obtain sensitivity better than the Standard Quantum Limit (SQL) using significantly lower amount of optical pumping energy than in traditional (extracavity) schemes.

In the article [6] the last scheme was analyzed in detail. It was shown that it is feasible using current technology to beat the SQL by the factor of ~ 2 using high-quality cryogenic microwave resonators. The main limiting factor here is the microwave resonator relaxation time achievable in the real experiment, which must be large due to the condition (1). It is necessary to note that eigenfrequency of one of the cavities have to be dependent on the position of the test mass, which limits greatly achievable quality factors of the microwave resonators (see brief analysis in the section V of the article [6]).

In that article it was also proposed the adaptation of this scheme into the optical band, which can be used directly in the extracavity topology of the gravitational-wave antennae and which also allows to obtain sensitivity better than the SQL. It is based on the fact that using the best modern high-reflectivity mirrors [7], the values as long as $1 \div 10$ s can be obtained for the Fabry-Perot cavities with length $L \gtrsim 10^5$ cm typical for the interferometric gravitational-wave antennae. Therefore, condition (1) can be fulfilled relatively easily for the typical frequencies of the gravitational-wave signal $\Omega_{\text{signal}} \sim 10^2 \div 10^3 \text{ s}^{-1}$.

This idea was developed in the articles [8, 9]. In these articles different topologies and regimes of the quantum speedmeter scheme based on large-scale Fabry-Perot cavities was analyzed in detail. It was shown that sensitivity several times better than the SQL can be achieved at the current technological level.

However, these schemes has serious disadvantages: they require huge value of the pumping power or an additional large-scale Fabry-Perot cavity.

Another topology of the interferometer, which is sensitive to velocity instead of the test masses position is a zero-area Sagnac interferometer [10]. Prototypes of such a device have been built and the characteristic frequency response proportional to the observation frequency Ω was demonstrated [11, 12]. In the article [13] a quantum-mechanical study of Sagnac interferometers was carried out.

Traditionally in zero-area Sagnac interferometers optical delay lines or ring cavities are used instead of Fabry-Perot cavities, and it is these topologies was considered in the paper [13]. At the same time, Fabry-Perot cavities are more convenient for the kilometer-scale interferometers from the technological point of view.

In this paper the new version of the quantum speedmeter which combines the zero-area Sagnac interferometer with Fabry-Perot cavities is presented. Only two such cavities are used and therefore only minimal changes in the standard Fabry-Perot/Michelson topology of the laser gravitational-wave antennae are required in the proposed scheme.

In the section 2 general properties of all quantum speedmeter schemes are considered. The main goal of this section is to show, that the mentioned above cross-correlation between the measurement noise and back-action noise is necessary in order to evade SQL in this scheme due to the subtle difference between momentum and velocity of a free mass.

In the section 3 the Sagnac/Fabry-Perot quantum speedmeter scheme is analyzed and the sensitivity of this scheme which can be obtained using contemporary technologies is estimated.

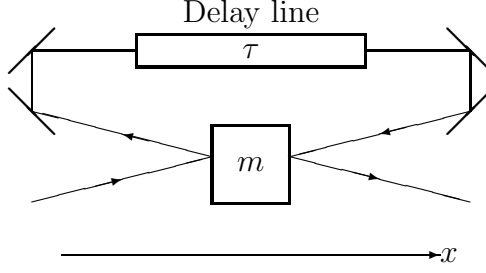


Figure 1: Gedanken scheme of the quantum speedmeter

2 General properties of the Quantum Speedmeter

2.1 The simplest gedanken scheme

Simple gedanken scheme illustrating the idea and the main properties of the quantum speedmeter is presented in Fig. 1.

Here an optical pulse is reflected from the left side of the test mass m , then passes through the delay line and then is reflected again from the other side of the test mass. If test mass does not move then the total phase shift of the optical pulse does not depend on its initial position. However if it does move then there will be some phase shift

$$\delta\varphi = \frac{2\omega_o\bar{v}\tau}{c}, \quad (2)$$

where τ is the time interval between two reflections and \bar{v} is the velocity of the test mass during this interval. Therefore, monitoring the phase of the output light beam it is possible to measure the velocity \bar{v} with precision

$$\Delta\bar{v}_{\text{meas}} = \frac{c\Delta\varphi}{2\omega_o\tau}, \quad (3)$$

where $\Delta\varphi$ is the phase uncertainty of the optical pulse.

During this procedure the test mass obtains two equal kicks in opposite directions. Therefore, its velocity *after* the measurement is not perturbed. However, velocity *between* the kicks is perturbed by the value

$$\Delta v_{\text{pert}} = \frac{2\Delta\mathcal{E}}{mc}, \quad (4)$$

where $\Delta\mathcal{E}$ is the energy uncertainty of the light pulse.

From this follow two conclusions. First, position of the test mass after the measurement is perturbed by the value

$$\Delta x_{\text{pert}} = \frac{2\Delta\mathcal{E}\tau}{mc}. \quad (5)$$

It can be obtained from the formulas (3) and (5) that

$$\Delta \bar{v}_{\text{meas}} \Delta x_{\text{pert}} = \frac{\Delta \mathcal{E} \Delta \varphi}{2m\omega_o} \geq \frac{\hbar}{2m}, \quad (6)$$

in accord with the uncertainty relation.

Second, measurement error for the *initial* value of the velocity of the test mass contains term (4) in addition to (3). Simple optimization of these two terms gives the value which is exactly equal to the SQL:

$$\Delta v_{\text{SQL}} = \sqrt{\frac{\hbar}{m\tau}}. \quad (7)$$

In the article [4] it was shown, however, that this additional error can be eliminated by using cross-correlation between the measurement error and perturbation. In the scheme described above this cross-correlation can be obtained either by using non-classical quantum state of the light pulse with correlated phase and energy, or by detecting the output light beam by homodyne detector with optimally chosen phase of the local oscillator. In both cases the measurement error for the initial value of velocity will be equal to

$$\Delta v_{\text{opt}} = \frac{\hbar c}{2\tau \Delta \mathcal{E}}. \quad (8)$$

2.2 Single velocity measurement

The general abstract scheme of the quantum speedmeter represents the direct generalization of the example considered above. Let again m be a free mass which velocity v have to be measured. Let \mathcal{N} be the observable of the meter, which provide its coupling with the test mass, and $\alpha(t)$ is the coupling factor, $\alpha(t) = 1$ when the meter is on and $\alpha(t) = 0$ when the meter is off. Suppose also that we can neglect the variable \mathcal{N} self evolution during the measurement (this is a reasonable assumption because in real schemes of the speedmeter, and in the gedanken example considered above, the number of quanta in e.m. wave corresponds to this variable). Due to this assumption, we can set the Hamiltonian of the meter equal to zero (see also the article [14]).

Lagrangian of this system can be presented as

$$\mathcal{L} = \frac{mv^2}{2} - \alpha(t)v\mathcal{N}, \quad (9)$$

Therefore, momentum of the mass m is equal to

$$p = \frac{\partial \mathcal{L}}{\partial v} = mv - \alpha(t)\mathcal{N}, \quad (10)$$

and the Hamiltonian of the system is equal to

$$\mathcal{H} = pv - \mathcal{L} = \frac{[p + \alpha(t)\mathcal{N}]^2}{2m}. \quad (11)$$

The output signal of the meter is represented by observable Φ canonically conjugated to \mathcal{N} (if \mathcal{N} corresponds to the number of quanta in e.m. wave then Φ corresponds to the phase of this wave). Evolution of the test object position x and the observable Φ is described by the equations

$$\frac{d\hat{x}(t)}{dt} \equiv \hat{v}(t) = \frac{\hat{p} + \alpha(t)\hat{\mathcal{N}}}{m}, \quad (12)$$

$$\frac{d\hat{\Phi}(t)}{dt} = \alpha(t)\hat{v}(t). \quad (13)$$

Solution of these equations can be presented in the following form:

$$\hat{x}(\tau) = \hat{x}(0) + \frac{\hat{p}\tau}{m} + \frac{\hat{\mathcal{N}}\tau}{m}, \quad (14)$$

$$\hat{\Phi}(\tau) = \hat{\Phi}(0) + \hat{v}\tau = \hat{\Phi}(0) + \frac{\hat{\mathcal{N}}\tau}{m} + \hat{v}_{\text{init}}\tau, \quad (15)$$

where $\bar{v} = (p + \mathcal{N})/m$ is the value of velocity when the meter is turned on, $v_{\text{init}} = p/m$ is the initial value of the velocity, and τ is the duration of the measurement.

Therefore, the momentum of the test mass is not perturbed and its velocity is perturbed during the measurement by the value of $\alpha(t)\mathcal{N}/m$, but returns to the initial value after the end of the measurement [see formula (12)]. Perturbation of the position of the test mass after the measurement is proportional to the uncertainty of observable \mathcal{N} [see formula (14)]:

$$\Delta x_{\text{pert}} = \frac{\Delta \mathcal{N} \tau}{m}. \quad (16)$$

By measuring variable Φ after the interaction of the meter with the test object one can estimate the *perturbed* value of velocity \bar{v} with precision [see formula (15)]

$$\Delta \bar{v}_{\text{meas}} = \frac{\Delta \Phi}{\tau}. \quad (17)$$

It follows from the last two formulas, that

$$\Delta x_{\text{pert}} \Delta \bar{v}_{\text{meas}} = \frac{\Delta \Phi \Delta \mathcal{N}}{m} \geq \frac{\hbar}{2m}. \quad (18)$$

At the same time, the measurement error for the *initial* unperturbed value of the velocity $v_{\text{init}} = p/m$ depends on both $\Delta \Phi$ and $\Delta \mathcal{N}$ and “naive” optimization gives that the precision is limited by the value (7).

However, using cross-correlation between the measurement error and back-action it is possible to measure v_{init} with arbitrary high precision. Similar to the previous example, this cross-correlation can be implemented whether by preparation of the meter in the initial state with well-defined value of the combination $\Phi(0) + \mathcal{N}\tau/m$, or by monitoring the variable $\Phi(\tau) - \mathcal{N}\tau/m$ instead of $\Phi(\tau)$. In both cases it is possible to measure the initial velocity with precision

$$\Delta v_{\text{opt}} = \frac{\hbar}{2\tau \Delta \mathcal{N}}. \quad (19)$$

2.3 Continuous monitoring of the velocity

Convenient method for consideration the continuous monitoring of the velocity of the quantum test body is based on *linear quantum meter* approach [3, 14]. Let a classical signal force F_{signal} which has to be detected acts on a quantum test mass m . Suppose that the velocity of test mass $v(t)$ is monitored by the quantum speed meter. Output signal of such a meter is proportional to a sum of the current value of velocity and the measurement noise $v_{\text{fluct}}(t)$:

$$\tilde{v}(t) = \hat{v}(t) + \hat{v}_{\text{fluct}}(t), \quad (20)$$

At the same time, the meter perturbs the test mass by means of the random force $F_{\text{fluct}}(t)$. In the case of speedmeter, this force have not to perturb momentum of the test object. It can be shown that in this case the force can be presented in the form

$$\hat{F}_{\text{fluct}}(t) = \frac{d\hat{p}_{\text{fluct}}(t)}{dt}, \quad (21)$$

where $\hat{p}_{\text{fluct}}(t)$ is some another random function. Therefore,

$$\hat{v}(t) = \hat{v}_{\text{init}} + \frac{1}{m} \left(\int_0^t F_{\text{signal}}(t') dt + \hat{p}_{\text{fluct}}(t) \right). \quad (22)$$

It follows from the equations (20) and (22) that signal to noise ratio for such system is equal to:

$$\frac{s}{n} = \int_{-\infty}^{\infty} \frac{|F_{\text{signal}}(\Omega)|^2}{S_{\text{total}}(\Omega)} \frac{d\Omega}{2\pi}, \quad (23)$$

where Ω is the observation frequency and

$$S_{\text{total}}(\Omega) = \Omega^2(m^2 S_v + 2m S_{vp} + S_p), \quad (24)$$

is the spectral density of the total net noise of the meter. Here S_v and S_p are the spectral densities of the noises $v_{\text{fluct}}(t)$ and $p_{\text{fluct}}(t)$ correspondingly, and S_{vp} is their cross spectral density, which satisfy the uncertainty relation

$$S_v S_p - S_{vp}^2 \geq \frac{\hbar^2}{4}. \quad (25)$$

Suppose first that $S_{vp} = 0$ (there is no cross-correlation). It is easy to show that in this case

$$S_{\text{total}}(\Omega) \geq \hbar m \Omega^2 \quad (26)$$

for all possible values of S_v and S_p . This value exactly corresponds to the spectral form of the SQL [6].

However, if S_{vp} is chosen in the optimal way:

$$S_{vp} = -\frac{S_p}{m}, \quad (27)$$

then the total noise is limited only by the condition

$$S_{\text{total}}(\Omega) \geq \frac{\hbar^2 \Omega^2 m^2}{4 S_p}, \quad (28)$$

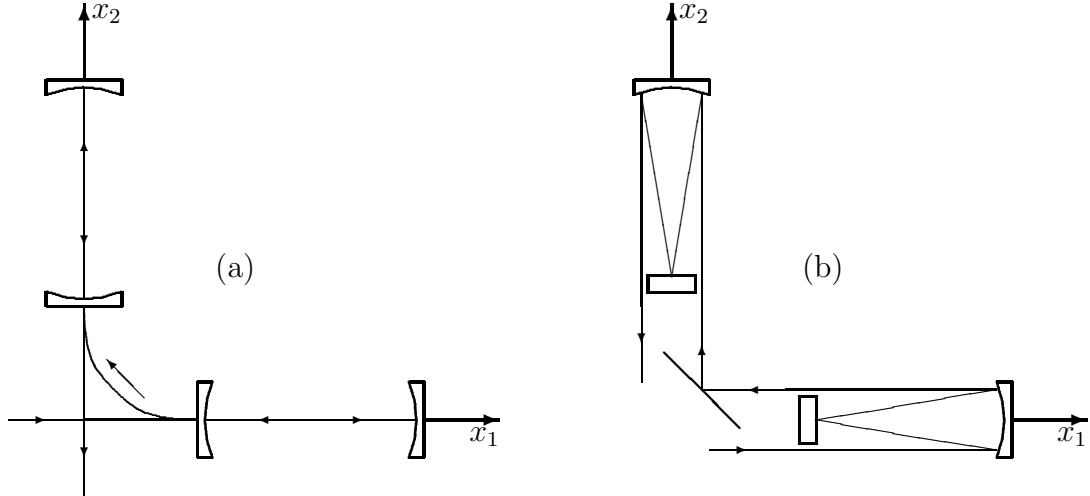


Figure 2: The idea of the optical speedmeter

and can be made arbitrary small if sufficient value of S_p is provided.

It is important that the cross-correlation (27) does not depend on the observation frequency. Therefore it can be implemented easily using homodyne detector with fixed value of the local oscillator phase. The variation measurement [15, 16] also allows to obtain sensitivity better than the SQL using the back-action and measurement noises cross-correlation. However, in the latter case sophisticated time- or frequency-dependence of the local oscillator phase is required in order to overcome the SQL in the wide band.

3 The optical speedmeter

3.1 The idea of the optical speedmeter

Suppose that we are managed, by some means, to separate output light beams from the input ones for both of the Fabry-Perot cavities used in the standard topology of the laser gravitational-wave antennae. One of the possible designs which allows to do it will be presented below (see Fig. 4). In this case it is possible to direct the light beam first to the one of the Fabry-Perot cavities and then to the second one as it is shown in Fig. 2(a). In principle, delay lines can be used in this scheme too and they allow to create “round-robin” passage of the pumping beam through the both arms more easily [see Fig. 2(b)], as it was proposed in the article [13]. However, Fabry-Perot cavities are more convenient for the kilometer-scale interferometers from the technological point of view. Therefore, Fabry-Perot cavities will be considered in this article.

Using rather crude but qualitatively correct approximation, phase of the output beam can be presented in the following form (the rigorous analysis is provided in the Appendix A):

$$\varphi_{\text{out}}(t) = \varphi_{\text{in}}(t) + \frac{2\omega_o\tau^*}{L} [2\bar{x}_+(t) + \bar{v}_-(t)\tau^*], \quad (29)$$

where

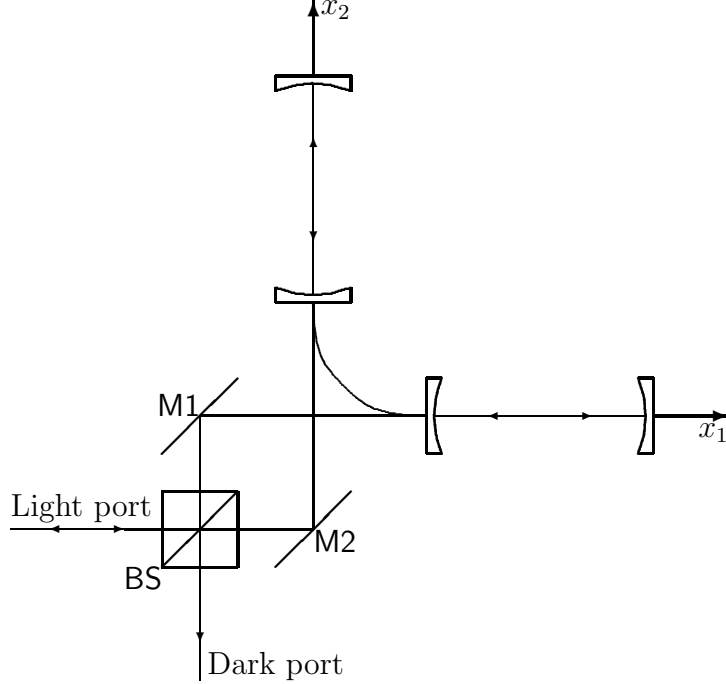


Figure 3: The conceptual design of the optical speedmeter

$$\begin{aligned}\bar{x}_+(t) &= \frac{x_+(t) + x_+(t - \tau^*)}{2}, \\ \bar{v}_-(t) &= \frac{x_-(t) - x_-(t - \tau^*)}{\tau^*},\end{aligned}\tag{30}$$

and

$$x_+ = \frac{x_1 + x_2}{2}, \quad x_- = \frac{x_1 - x_2}{2}.\tag{31}$$

Therefore, this scheme provides information about the velocity of the differential (anti-symmetric) motion of the end mirrors and about the position x_+ which corresponds to the symmetric motion.

In the gravitational-wave antennae the anti-symmetric mode is coupled with the gravitational-wave signal. In order to eliminate information about the position x_+ (the presence of this information, as it can be easily shown, does not permit to obtain sensitivity better than the SQL), two optical beams have to be used. One of them must “visit” the Fabry-Perot cavities in the clockwise order, as it is shown in Fig. 2 and the second one in the counter-clockwise order. Then the phase difference of these beams has to be measured. This modification allows also to protect the scheme from the frequency instability of the input laser beam.

The measurement of the phase difference of these two beams can be performed exactly in the same way as in the standard topology of the gravitational-wave antennae (see Fig. 3). Here beam

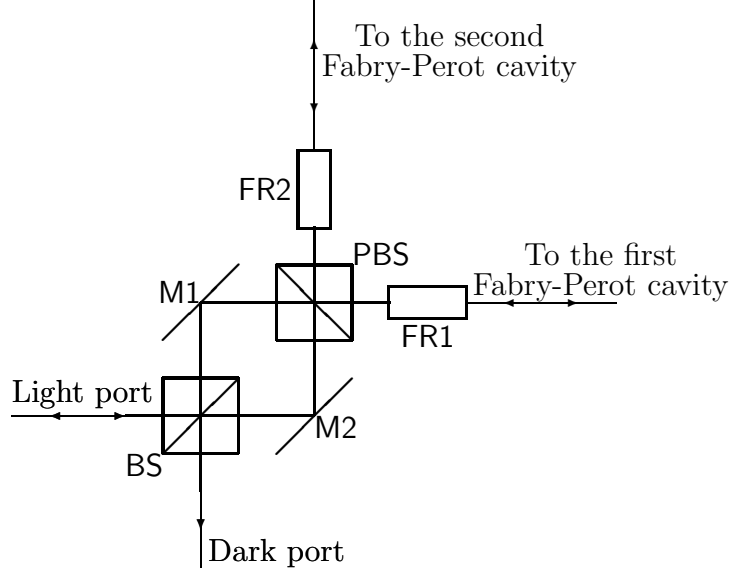


Figure 4: A possible design of the central station of the optical speedmeter

from the pumping laser is divided into two beams by the beam splitter. One of these beams leaves the beam splitter from the top, is reflected from the auxiliary mirror **M1**, from the right and then the upper Fabry-Perot cavities, and returns to the beam splitter from the right side. The second beam goes in the opposite direction. If the end mirrors of the Fabry-Perot cavities do not move then both beams gain equal phase shifts and all optical power returns to the pumping laser. However, the differential motion of the end mirrors will produce differential phase shift in both beams, proportional to the speed of this motion. In this case the part of pumping power will be splitted to the dark port and registered by the detector.

One of the possible designs of the central station for the optical speedmeter scheme is presented in Fig. 4.¹ Here **BS** is the ordinary 50%/50 beam splitter, **PBS** is the polarization beam splitter, and **FR1**, **FR2** are the Faraday rotators which rotate polarization of the light which pass through them by 45° .

Suppose that **PBS** reflects the light with vertical (90°) polarization and is transparent for the light with horizontal (0°) polarization. In this case the pumping laser has to generate horizontally polarized beam.

Consider, for example, the beam which goes from the **BS** to the upper direction. It is reflected from the auxiliary mirror **M1**, passes through the **PBS** and then through the **FR1**, and goes to the first Fabry-Perot cavity having 45° polarization. After reflection from the Fabry-Perot cavity, it passes through the **FR1** for the second time. At this moment it has vertical polarization and hence is reflected from **PBS** and goes to the upper direction. Then it passes through **FR2**, is reflected from the second Fabry-Perot cavity, passes through **FR2** for the second time (now it has horizontal polarization again), passes through the **PBS**, is reflected from the second auxiliary mirror **M2**, and

¹This scheme should be considered as an example only; it is very possible that better implementations of the idea presented here are exist. In particular, quarter-wave plates can be used instead of the Faraday rotators and, correspondingly, the circular polarization instead of the linear one [17].

returns to the main beam splitter BS from the right direction.

3.2 Sensitivity of the optical speedmeter

In the Appendix A the explicit values of the spectral densities introduced in the section 2.3 are calculated for the scheme of the optical speedmeter described above. Here we consider for simplicity only the particular case when observation frequency Ω small compared to the half-bandwidth of the Fabry-Perot cavities γ . In this case, these spectral densities are equal to [see the formulas (86, 87, 88)]:

$$S_v = \frac{\hbar L^2 \gamma^4}{64 \omega_o w \cos^2 \varphi}, \quad (32)$$

$$S_p = \frac{16 \hbar \omega_o w}{L^2 \gamma^4}, \quad (33)$$

$$S_{vp} = \frac{\hbar}{2} \tan \varphi, \quad (34)$$

where w is the pumping power, and φ is the phase shift between the pumping beam and the local oscillator beam.

It follows from the conditions (27) and (28) that the optimal value of φ is equal to

$$\varphi = -\arctan \frac{32 \omega_o w}{m L^2 \gamma^4}, \quad (35)$$

and corresponding optimal spectral density of the total noise is described by the formula

$$\xi^2 \equiv \frac{S_{\text{total}}(\Omega)}{S_{\text{SQL}}(\Omega)} = \frac{m L^2 \gamma^4}{64 \omega_o w}. \quad (36)$$

where

$$S_{\text{SQL}}(\Omega) = \hbar m \Omega^2 \quad (37)$$

is the spectral density of the total noise which corresponds to the SQL [6].

Formula (36) has the structure typical for all interferometric meters (see, for example, articles [15, 16, 18]), which originates from the Energetic Quantum Limit [3, 19]. Due to this limitation, in order to obtain the sensitivity equal to the SQL ($\xi = 1$), the pumping power has to be close to the value planned for the contemporary large-scale gravitational-wave antennae and in order to obtain better sensitivity it is necessary to increase pumping power proportionally to ξ^{-2} .

Consider, for example, values of the parameters typical for the gravitational-wave antenna LIGO-I: $m = 10 \text{ Kg}$, $L = 4 \text{ Km}$, $\gamma = 10^3 \text{ s}^{-1}$ and $\omega_o = 2 \cdot 10^{15} \text{ s}^{-1}$. In this case

$$\xi^2 \approx \frac{1.25 \text{ KWt}}{w}. \quad (38)$$

It have to be noted, that this value of the pumping power can be reduced using the power recycling, exactly as it is planned for the standard topology of the LIGO. However, power circulating *inside* the interferometer remains the same. Formula (38) in this case describes the power passing through the beam splitter.

4 Conclusion

Sensitivity of the scheme of the optical speedmeter considered here is typical for schemes with traditional (extracavity) topology. If pumping beam in coherent quantum state is used then it is necessary about one kilowatt (without power recycling) of the optical power in order to reach the Standard Quantum Limit, and the necessary pumping power depends on the required sensitivity as h^{-2} , where h is the signal amplitude which has to be detected.

However, this scheme has the following advantages in comparison with other proposed schemes with extracavity topology (see, for example, references [6, 15, 16, 20, 21]):

- It allows to obtain sensitivity better than the Standard Quantum Limit in wide band (the bandwidth is limited by the bandwidth of the Fabry-Perot cavities only).
- It does not require exact information about the shape and arrival time of the signal.
- It does not require any large-scale modifications of the standard topology of the laser interferometric antennae.
- It does not require non-classical state of the pumping power (however, using squeezed quantum state it is possible to reduce the value of the pumping power)

Therefore, considered scheme looks as the promising option for the first step beyond the Standard Quantum Limit.

Acknowledgments

Author thanks V.B.Braginsky and S.L.Danilishin for useful remarks.

This paper was supported in part by US National Science Foundation, by the Russian Foundation for Basic Research, and by the Russian Ministry of Industry and Science.

A Spectral densities of the noises of the optical speedmeter

A.1 Intermediate formulas

A.1.1 Single moving mirror

Consider first a single moving mirror with reflection $R = -1$. Let $x(t)$ be the current position of the mirror and a, b are the annihilation operators corresponding to the incident and reflected beams (see Fig. 5(a)).

Suppose that the incident beam can be presented as a sum of a strong classical monochromatic wave with frequency ω_o and small quantum term, which we refer below to as “zeroth approximation” and “first approximation”, correspondingly:

$$\hat{E}_a(t) = E_0(\omega_o)Ae^{-i\omega_o t} + \int_0^\infty E_0(\omega)\hat{a}(\omega)e^{-i\omega t}\frac{d\omega}{2\pi} + \text{h.c.} . \quad (39)$$

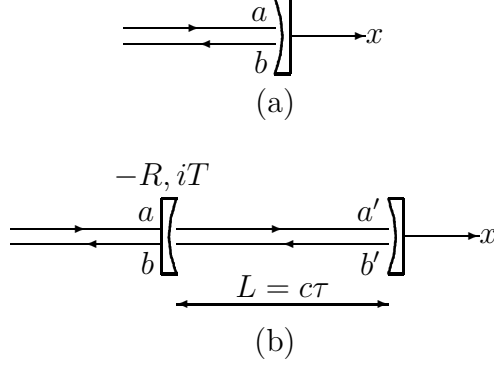


Figure 5: Reflection from a moving mirror (a) and a Fabry-Perot cavity (b)

Here

$$E_0(\omega) = \sqrt{\frac{2\pi\hbar\omega}{\mathcal{A}c}} \quad (40)$$

is the normalization factor, \mathcal{A} is the cross-section area of the beam, and h.c. stands for “Hermitian conjugate”. This value of the normalization factor corresponds to the commutator

$$[\hat{a}(\omega), \hat{a}^+(\omega')] = 2\pi\delta(\omega - \omega'). \quad (41)$$

Neglecting relativistic terms proportional to $1/c^2$ the reflected beam can be presented in the following form:

$$\hat{E}_b(t) \approx -\frac{1 - \hat{x}(t)/c}{1 + \hat{x}(t)/c} \hat{E}_a(t - 2x(t)/c) \approx \hat{E}_a(t) - \frac{1}{c} \frac{d\hat{x}(t)}{dt} \hat{E}_a(t). \quad (42)$$

Taking into account formula (39) expression (42) can be rewritten as:

$$\hat{E}_b(t) = E_0(\omega_o) B e^{-i\omega_o t} + \int_0^\infty E_0(\omega) \hat{b}(\omega) e^{-i\omega t} \frac{d\omega}{2\pi} + \text{h.c.}, \quad (43)$$

where

$$B = -A,$$

$$\hat{b}(\omega) = -\hat{a}(\omega) - 2i\kappa(\omega)A\hat{x}(\omega_o - \omega), \quad (44)$$

$$\kappa(\omega) = \frac{\sqrt{\omega_o\omega}}{c}, \quad (45)$$

and

$$\hat{x}(\Omega) = \int_{-\infty}^\infty \hat{x}(t) e^{-i\Omega t} \frac{d\Omega}{2\pi} \quad (46)$$

is the spectrum of the $\hat{x}(t)$.

A.1.2 Reflection from a Fabry-Perot cavity

Suppose then that the second mirror with the reflection $-R$ and transmittance iT ($R^2 + T^2 = 1$) is added to the first one forming a Fabry-Perot cavity with the length $L = c\tau_1$ [see Fig. 5(b)].

Using the same representation (39) as in the previous subsection, equation for the field amplitudes can be written as the following:

$$\begin{aligned} B &= -RA + iTB'e^{i\omega_o\tau_1}, \\ A' &= iTAe^{i\omega_o\tau_1} - RB'e^{2i\omega_o\tau_1}, \\ B' &= -A', \end{aligned} \quad (47)$$

$$\begin{aligned} \hat{b}(\omega) &= -R\hat{a}(\omega) + iT\hat{b}'(\omega)e^{i\omega\tau_1}, \\ \hat{a}'(\omega) &= iT\hat{a}(\omega)e^{i\omega\tau_1} - R\hat{b}'(\omega)e^{2i\omega\tau_1}, \\ \hat{b}'(\omega) &= -\hat{a}'(\omega) - 2i\kappa(\omega)A'\hat{x}(\omega_o - \omega). \end{aligned} \quad (48)$$

Solution of these equations is equal to:

$$\begin{aligned} B &= \mathcal{R}(\omega_o)A, \\ A' &= -B' = \mathcal{T}(\omega_o)A, \end{aligned} \quad (49)$$

$$\hat{b}(\omega) = \mathcal{R}(\omega)\hat{a}(\omega) + \kappa(\omega)A'\mathcal{S}(\omega)\hat{x}(\omega_o - \omega), \quad (50)$$

$$\hat{a}'(\omega) - \hat{b}'(\omega) = 2\mathcal{T}(\omega)\hat{a}(\omega) + \kappa(\omega)A'\mathcal{W}(\omega)\hat{x}(\omega_o - \omega), \quad (51)$$

where

$$\begin{aligned} \mathcal{R}(\omega) &= \frac{\mathcal{L}^*(\omega)}{\mathcal{L}(\omega)}, & \mathcal{S}(\omega) &= \frac{2\sqrt{\Gamma}}{\mathcal{L}(\omega)}, \\ \mathcal{T}(\omega) &= \frac{i\sqrt{\Gamma}}{\mathcal{L}(\omega)}, & \mathcal{W}(\omega) &= 2i\frac{\mathcal{L}'(\omega)}{\mathcal{L}(\omega)}, \end{aligned} \quad (52)$$

and

$$\begin{aligned} \mathcal{L}(\omega) &= \Gamma \cos \omega\tau_1 - i \sin \omega\tau_1, \\ \mathcal{L}'(\omega) &= \cos \omega\tau_1 - i\Gamma \sin \omega\tau_1, \\ \Gamma &= \frac{1-R}{1+R}. \end{aligned} \quad (53)$$

These formulas can be simplified if the pumping frequency is equal to one of the eigenfrequencies of the Fabry-Perot cavity, $\omega_o\tau_1 = 2\pi n$, and the observation frequency is relatively small, $\Omega\tau_1 \ll 1$. In this case

$$\begin{aligned}
\mathcal{R}(\omega_o + \Omega) &\approx \frac{\gamma + i\Omega}{\gamma - i\Omega}, & \mathcal{S}(\omega_o + \Omega) &\approx \frac{2\sqrt{\gamma/\tau_1}}{\gamma - i\Omega}, \\
\mathcal{T}(\omega_o + \Omega) &\approx \frac{\sqrt{\gamma/\tau_1}}{\gamma - i\Omega}, & \mathcal{W}(\omega_o + \Omega) &\approx \frac{2i}{\tau_1} \frac{1}{\gamma - i\Omega},
\end{aligned} \tag{54}$$

where $\gamma = \Gamma/\tau_1$ is the half-bandwidth of the cavity.

A.1.3 Pondermotive force

The formula (51) allows to calculate the pondermotive force acting on the moving mirror in a Fabry-Perot cavity. This force is equal to

$$F(t) = \frac{\mathcal{A}}{4\pi} \left[\overline{E_{a'}^2(t)} + \overline{E_{b'}^2(t)} \right], \tag{55}$$

where overline means averaging over time larger than the period of the optical oscillations $2\pi/\omega_o$. This force can be presented as a sum of the large constant force

$$F_0 = \frac{2W}{c} = \frac{2w}{c\Gamma}, \tag{56}$$

where $W = |A'|^2/c$ is the mean value of the power circulating in the cavity and $w = |A|^2/c$ is the mean power of the incident beam, and the fluctuating force

$$\begin{aligned}
\hat{F}(t) &= \hbar A'^* \int_0^\infty \kappa(\omega) [\hat{a}'(\omega) - \hat{b}'(\omega)] e^{i(\omega_o - \omega)t} \frac{d\omega}{2\pi} + \text{h.c.} \\
&= \hbar \int_0^\infty [2\kappa(\omega) A'^* \mathcal{T}(\omega) \hat{a}(\omega) + \kappa^2(\omega) |A'|^2 \mathcal{W}(\omega) \hat{x}(\omega_o - \omega)] e^{i(\omega_o - \omega)t} \frac{d\omega}{2\pi} + \text{h.c.} .
\end{aligned} \tag{57}$$

A.2 The optical speedmeter

A.2.1 General remarks and notations

The following notations will be used in this subsection (see Fig.6):

a_1 is the amplitude of the beam which goes from the main beam splitter **BS** to the right directions, is reflected from the mirror **M2**, passes through the polarization beam splitter **PBS**, and enters the upper Fabry-Perot cavity with 45° -polarization;

g_1 is the amplitude of this beam after the reflection from the upper Fabry-Perot cavity; it is reflected from the **PBS** and enters into the right Fabry-Perot cavity with 135° -polarization;

b_2 is the amplitude of this beam after the reflection from the right Fabry-Perot cavity; it passes through the **PBS** and returns to the **BS** from the upper direction;

a_2 , g_2 and b_1 describe the beam which goes in the opposite direction in the similar way;

$a'_1(45^\circ)$ and $a'_1(135^\circ)$ are the amplitudes pumped in the first (right) cavity by the beams a_2 and g_1 , correspondingly;

$a'_2(45^\circ)$ and $a'_2(135^\circ)$ are the amplitudes pumped in the second (upper) cavity by the beams a_1 and g_2 , correspondingly;

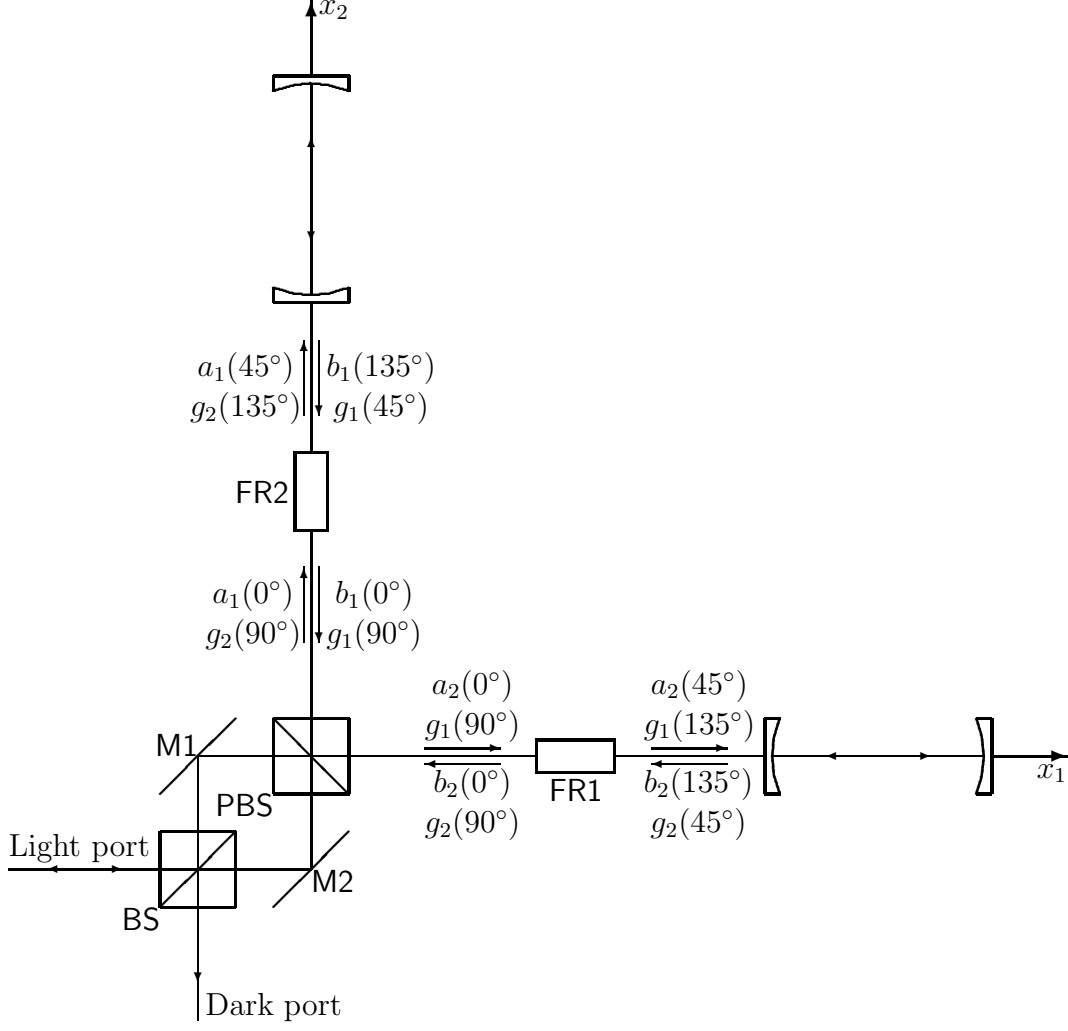


Figure 6: The optical speedmeter

a_3 corresponds to the beam which goes from the BS to the left direction (to the pumping laser), and b_4 — to the beam which goes from the laser to the BS;

a_4 corresponds to the beam which goes from the BS to the down direction (to the detector), and b_4 — to the beam which goes from the detector to the BS.

The main beam splitter BS is described by the following equations:

$$\begin{aligned} \hat{a}_1 &= -\frac{\hat{b}_3 + i\hat{b}_4}{\sqrt{2}}, & \hat{a}_2 &= -\frac{\hat{b}_3 - i\hat{b}_4}{\sqrt{2}}, \\ \hat{a}_3 &= -\frac{\hat{b}_1 + \hat{b}_2}{\sqrt{2}}, & \hat{a}_4 &= -i\frac{\hat{b}_1 - \hat{b}_2}{\sqrt{2}}. \end{aligned} \quad (58)$$

It is presumed here that there is the additional phase shift $\pi/2$ in the right port “1” of the beam splitter, which is necessary in order to provide the dark fringe regime (exactly as in the standard

topology).

A.2.2 Field amplitudes

In the zeroth approximation in addition to the equations (58) the following equations can be written:

$$B_{1,2} = G_{2,1}, \quad G_{1,2} = A_{1,2}, \quad (59)$$

$$A'_{1,2}(45^\circ) = \frac{iA_{2,1}}{\sqrt{\Gamma}}, \quad A'_{1,2}(135^\circ) = \frac{iG_{1,2}}{\sqrt{\Gamma}}. \quad (60)$$

Solving this set of equations and taking into account that $B_4 = 0$ (there is no pumping in the dark port), we obtain that

$$A_3 = B_3, \quad A_4 = 0, \\ A'_1(45^\circ) = A'_1(135^\circ) = A'_2(45^\circ) = A'_2(135^\circ) \equiv A' = -\frac{iB_3}{\sqrt{2\Gamma}}. \quad (61)$$

In the first approximation the following equation can be obtained from the formula (50):

$$\hat{b}_{1,2}(\omega) = \mathcal{R}(\omega)\hat{g}_{2,1}(\omega) + \varkappa(\omega)A'_{2,1}(135^\circ)\mathcal{S}(\omega)\hat{x}_{2,1}(\omega_o - \omega), \\ \hat{g}_{1,2}(\omega) = \mathcal{R}(\omega)\hat{a}_{1,2}(\omega) + \varkappa(\omega)A'_{2,1}(45^\circ)\mathcal{S}(\omega)\hat{x}_{2,1}(\omega_o - \omega). \quad (62)$$

Solution of the equations (58,62) is equal to:

$$\hat{b}_{1,2}(\omega) = \mathcal{R}^2(\omega)\hat{a}_{2,1}(\omega) + \varkappa(\omega)A'\mathcal{S}(\omega)[\mathcal{R}(\omega)\hat{x}_{1,2}(\omega_o - \omega) + \hat{x}_{2,1}(\omega_o - \omega)], \quad (63)$$

$$\hat{g}_{1,2}(\omega) = \mathcal{R}(\omega)\hat{a}_{1,2}(\omega) + \varkappa(\omega)A'\mathcal{S}(\omega)\hat{x}_{2,1}(\omega_o - \omega), \quad (64)$$

$$\hat{a}_4(\omega) = \mathcal{R}^2(\omega)\hat{b}_4(\omega) + i\sqrt{2}\varkappa(\omega)A'\mathcal{S}(\omega)[1 - \mathcal{R}(\omega)]\hat{x}_-(\omega). \quad (65)$$

A.2.3 Measurement noise

Using the formula (65), it can be shown that the output signal of the homodyne detector is proportional to²

$$\hat{\mathcal{I}}_{\text{detect}}(t) = \int_0^\infty \hat{a}_4(\omega)e^{i(\omega_o - \omega)t + i\phi_{\text{LO}}} \frac{d\omega}{2\pi} + \text{h.c.} = \hat{\mathcal{I}}_{\text{detect}}(t) + \hat{\mathcal{I}}_{\text{noise}}(t), \quad (66)$$

where ϕ_{LO} is the phase of the local oscillator,

$$\hat{\mathcal{I}}_{\text{noise}}(t) = \int_0^\infty \mathcal{R}^2(\omega)\hat{b}_4(\omega)e^{i(\omega_o - \omega)t + i\phi_{\text{LO}}} \frac{d\omega}{2\pi} + \text{h.c.} \quad (67)$$

²There is no factor $E_0(\omega) \propto \sqrt{\omega}$ in the next formula because the photocurrent is proportional not to the optical power but to the quanta flux.

is the noise,

$$\hat{\mathcal{I}}_{\text{signal}}(t) = \int_{-\infty}^{\infty} k(\Omega) \hat{x}(\Omega) e^{i\Omega t} \frac{d\Omega}{2\pi} \quad (68)$$

is the signal,

$$k(\Omega) = \frac{4i\sqrt{\omega_o}|B_3|\sin\Omega\tau_1[\sqrt{\omega_o-\Omega}e^{i\phi} + \sqrt{\omega_o+\Omega}e^{-i\phi}]}{c(\Gamma\cos\Omega\tau_1 + i\sin\Omega\tau_1)^2} \quad (69)$$

is the transmission factor and $\phi = \phi_{\text{LO}} + \arg B_3$ (note the factor $\sin\Omega\tau_1$).

If the pumping beam is in the coherent quantum state, then the spectral density of the noise $\hat{\mathcal{I}}_{\text{noise}}(t)$ is equal to

$$S_{\mathcal{I}}(\Omega) = 1, \quad (70)$$

In this case the spectral density of the measurement noise is equal to

$$S_x(\Omega) = \frac{S_{\mathcal{I}}(\Omega)}{|k(\Omega)|^2} = \frac{\hbar c^2(\Gamma^2 \cos^2 \Omega\tau_1 + \sin^2 \Omega\tau_1)^2}{16w \sin^2 \Omega\tau_1 |\sqrt{\omega_o + \Omega} e^{i\phi} + \sqrt{\omega_o - \Omega} e^{-i\phi}|^2}, \quad (71)$$

where $w = \hbar\omega_o|B_3|^2$ is the pumping power.

A.2.4 Back-action

Difference of the pondermotive (back action) forces which act on the distant mirrors of the Fabry-Perot cavities, is equal to

$$\hat{F}_-(t) = \hat{F}_1^{45^\circ}(t) + \hat{F}_1^{135^\circ}(t) - \hat{F}_2^{45^\circ}(t) - \hat{F}_2^{135^\circ}(t), \quad (72)$$

where [see the formulas (57, 61, 63, 64)]

$$\begin{aligned} \hat{F}_{1,2}^{45^\circ}(t) &= \hbar \int_0^\infty [2\kappa(\omega)A'^*\mathcal{T}(\omega)\hat{a}_{2,1}(\omega) + \kappa^2(\omega)|A'|^2\mathcal{W}(\omega)\hat{x}_{1,2}(\omega_o - \omega)] e^{i(\omega_o - \omega)t} \frac{d\omega}{2\pi} + \text{h.c.}, \\ \hat{F}_{1,2}^{135^\circ}(t) &= \hbar \int_0^\infty [2\kappa(\omega)A'^*\mathcal{T}(\omega)\hat{g}_{1,2}(\omega) + \kappa^2(\omega)|A'|^2\mathcal{W}(\omega)\hat{x}_{1,2}(\omega_o - \omega)] e^{i(\omega_o - \omega)t} \frac{d\omega}{2\pi} + \text{h.c.} \end{aligned} \quad (73)$$

Taking into account formulas (61, 63, 64), we obtain that

$$\hat{F}_-(t) = \hat{F}_{\text{fluct}}(t) + \hat{F}_{\text{dyn}}(t), \quad (74)$$

where

$$\hat{F}_{\text{fluct}}(t) = -2\frac{\hbar B_3^*}{\sqrt{\Gamma}} \int_0^\infty \kappa(\omega)\mathcal{T}(\omega)[1 - \mathcal{R}(\omega)]\hat{b}_4(\omega)e^{i(\omega_o - \omega)t} \frac{d\omega}{2\pi} + \text{h.c.} \quad (75)$$

is the fluctuational back action and

$$\begin{aligned}\hat{F}_-(t) &= 2\frac{\hbar|B_3|^2}{F} \int_0^\infty \varkappa^2(\omega) [\mathcal{W}(\omega) - \mathcal{S}(\omega)\mathcal{T}(\omega)] \hat{x}_-(\omega_o - \omega) e^{i(\omega_o - \omega)t} \frac{d\omega}{2\pi} + \text{h.c.} \\ &= - \int_{-\infty}^\infty K(\Omega) \hat{x}_-(\Omega), \quad (76)\end{aligned}$$

is the dynamic back action. The factor $K(\Omega)$ (the pondermotive rigidity) is equal to

$$K(\Omega) = -\frac{8w\Omega}{c^2 F} \frac{(1 + F^2) \cos \Omega\tau_1 \sin \Omega\tau_1 + i\Omega \sin^2 \Omega\tau_1}{(F \cos \Omega\tau_1 + i \sin \Omega\tau_1)^2} \approx (\text{if } \Omega\tau_1 \ll 1) \approx \frac{8w}{L^2 \gamma} \frac{(i\Omega)^2}{(\gamma + i\Omega)^2}. \quad (77)$$

This is a very small value: if, for example, $w = 1\text{KWt}$, $L = 4\text{Km}$, and $\gamma \sim \Omega \sim 10^3\text{s}^{-1}$ then $K \sim 10^{-3}\text{dyn/cm}^2$. Therefore, we can conclude that the dynamic back action is practically absent in this scheme.

If the pumping field is in the coherent quantum state then the spectral density of the fluctuational force (75) is equal to

$$S_F(\Omega) = \frac{16\hbar\omega_o w}{c^2} \frac{\sin^2 \Omega\tau_1}{(F^2 \cos^2 \Omega\tau_1 + \sin^2 \Omega\tau_1)^2}, \quad (78)$$

and the cross-correlation spectral density of the noises $\hat{\mathcal{I}}_{\text{noise}}$ and $\hat{F}_{\text{fluct}}(t)$ is equal to

$$S_{\mathcal{IF}}(\Omega) = \frac{2\hbar\sqrt{\omega_o}|B_3| \sin \Omega\tau_1 [\sqrt{\omega_o + \Omega} e^{i\phi} - \sqrt{\omega_o - \Omega} e^{-i\phi}]}{c(F \cos \Omega\tau_1 - i \sin \Omega\tau_1)^2}. \quad (79)$$

Therefore, cross-correlation spectral density for the measurement noise and the back-action noise is equal to

$$S_{xF}(\Omega) = \frac{S_{\mathcal{IF}}(\Omega)}{k^*(\Omega)} = \frac{i\hbar}{2} \frac{\sqrt{\omega_o + \Omega} e^{i\phi} - \sqrt{\omega_o - \Omega} e^{-i\phi}}{\sqrt{\omega_o + \Omega} e^{i\phi} + \sqrt{\omega_o - \Omega} e^{-i\phi}}. \quad (80)$$

It have to be noted, that

$$S_x(\Omega)S_F(\Omega) - |S_{xF}(\Omega)|^2 = \frac{\hbar^2}{4}. \quad (81)$$

A.2.5 The spectral densities

It is easy to note that the formulas (71, 78, 80) can be simplified. Really, the observation frequency $\Omega \lesssim 10^3\text{s}^{-1}$ is much smaller than the pumping frequency $\omega_o \sim 10^{15}\text{s}^{-1}$. Therefore, the formulas (71, 80) can be rewritten in the following form:

$$S_x(\Omega) = \frac{\hbar c^2}{64\omega_o w \cos^2 \phi} \frac{(F^2 \cos^2 \Omega\tau_1 + \sin^2 \Omega\tau_1)^2}{\sin^2 \Omega\tau_1}, \quad (82)$$

$$S_{xF}(\Omega) = -\frac{\hbar}{2} \tan \phi. \quad (83)$$

Then, in the real gravitational-wave antennae, $\tau_1 \lesssim 10^{-5} s$, and hence $\Omega\tau_1$ is also a small parameter. This allows to further simplify the formulas (78, 83):

$$S_x(\Omega) = \frac{\hbar L^2}{64\omega_o w \cos^2 \phi} \frac{(\gamma^2 + \Omega^2)^2}{\Omega^2}, \quad (84)$$

$$S_F(\Omega) = \frac{16\hbar\omega_o w}{L^2} \frac{\Omega^2}{(\gamma^2 + \Omega^2)^2}, \quad (85)$$

where $\gamma = \Gamma/\tau_1$. Therefore, the spectral densities S_v, S_p and S_{vp} can be presented in the following form:

$$S_v(\Omega) \equiv \Omega^2 S_x(\Omega) = \frac{\hbar L^2 (\gamma^2 + \Omega^2)^2}{64\omega_o w \cos^2 \phi}, \quad (86)$$

$$S_p(\Omega) \equiv \frac{S_F(\Omega)}{\Omega^2} = \frac{16\hbar\omega_o w}{L^2 (\gamma^2 + \Omega^2)^2}, \quad (87)$$

$$S_{vp}(\Omega) \equiv -S_{xF}(\Omega) = \frac{\hbar}{2} \tan \phi. \quad (88)$$

References

- [1] V.B.Braginsky, Yu.I.Vorontsov, F.Ya.Khalili, Sov. Phys. JETP **46**, 705 (1977).
- [2] Thorne K.S., R.W.P.Drever, C.M.Caves, M.Zimmerman, V.D.Sandberg, Physical Review Letters **40**, 667 (1978).
- [3] V.B.Braginsky, F.Ya.Khalili, *Quantum Measurement*, Cambridge University Press, 1992.
- [4] V. B. Braginsky, F. Ya. Khalili, Physics Letters A **147**, 251 (1990).
- [5] V.B.Braginsky, M.L.Gorodetsky, F.Ya.Khalili, Physics Letters A **246**, 485 (1998).
- [6] V.B.Braginsky, M.L.Gorodetsky F.Ya.Khalili and K.S.Thorne, Physical Review D **61**, 044002 (2000).
- [7] G.Rempe, R.Tompson, H.J.Kimble, Optics Letters **17**, 363 (1992).
- [8] P.Purdue, Physical Review D **66**, 022001 (2002).
- [9] P.Purdue, Yanbei Chen, gr-qc/0208049.
- [10] K-X.Sun, M.M.Fejer, E.Gustafson, D.Shoemaker, and R.L.Byer, Physical Review Letters **76**, 3055 (1996).
- [11] P.Beyersdorf, M.M.Fejer, and R.L.Byer, Optics Letters **24**, 1112 (1999).
- [12] S.Traeger, P.Beyersdorf, L.Goddard, E.Gustafson, M.M.Fejer, and R.L.Byer, Optics Letters **25**, 722 (2000).

- [13] Yanbei Chen, gr-qc/0208051.
- [14] V.B.Braginsky, M.L.Gorodetsky, F.Ya.Khalili, A.B.Matsko, K.S.Thorne and S.P.Vyatchanin, submitted to Physical Review D; gr-qc/0109003 (2002).
- [15] S. P. Vyatchanin, Physics Letters A **239**, 201 (1998).
- [16] H.J.Kimble, Yu.Levin, A.B.Matsko, K.S.Thorne and S.P.Vyatchanin, Physical Review D **65**, 022002 (2002).
- [17] Shanti Rao, *private communication*.
- [18] S. L. Danilishin, F. Ya. Khalili and S. P. Vyatchanin, Physics Letters A **278**, 123 (2000).
- [19] V.B.Braginsky, M.L.Gorodetsky, F.Ya.Khalili and K.S.Thorne, Energetic quantum limit in large-scale interferometers, in *Gravitational waves. Third Edoardo Amaldi Conference, Pasadena, California 12-16 July, ed. S.Meshkov, Melville NY:AIP Conf. Proc. 523*, pages 180–189, 2000.
- [20] F.Ya.Khalili, Physics Letters A **288**, 251 (2001).
- [21] A.Buonanno, Yanbei Chen, Physical Review D **65**, 042001 (2002).